



# Assessing the bioenergy potential of high-ash anaerobic sewage sludge using pyrolysis kinetics and thermodynamics to design a sustainable integrated biorefinery

José Luiz Francisco Alves<sup>1</sup> · Jean Constantino Gomes da Silva<sup>1</sup> · Mariana Pires Langer<sup>1</sup> · Luciane Batistella<sup>2</sup> · Michele Di Domenico<sup>3</sup> · Valdemar Francisco da Silva Filho<sup>1</sup> · Regina de Fátima Peralta Muniz Moreira<sup>1</sup> · Humberto Jorge José<sup>1</sup>

Received: 11 July 2020 / Revised: 10 September 2020 / Accepted: 16 September 2020 / Published online: 29 September 2020  
© Springer-Verlag GmbH Germany, part of Springer Nature 2020

## Abstract

A new opportunity for producing valuable biorefinery products can be found by integrating biochemical and thermochemical processing with municipal wastewater treatment. This study is the first to evaluate the kinetic triplet and thermodynamic parameters from the pyrolysis of typical Brazilian anaerobic sewage sludge performed in the framework of a multi-step solid-state process. The physicochemical characteristics of the anaerobic sewage sludge are comparable to those obtained from low-rank coals. The pyrolysis characteristics were analyzed by non-isothermal thermogravimetry under different heating rates (10, 25, 50, and 90 K min<sup>-1</sup>) in an inert atmosphere. Two devolatilization stages were distinguished from the active pyrolysis zone, with an average mass loss of 47.56 wt% (sum) in the range of 398–953 K. For each devolatilization stage, three isoconversional methods (Flynn–Wall–Ozawa, Kissinger–Akahira–Sunose, and Starink) were utilized to calculate the activation energy, and then the compensation effect method was applied to find the pre-exponential factor. The average activation energies calculated ranged from 113.7 to 117.3 kJ mol<sup>-1</sup> for the first stage and from 115.7 to 121.9 kJ mol<sup>-1</sup> for the second stage, with respective pre-exponential factors of  $7.39 \times 10^9 \text{ min}^{-1}$  and  $8.80 \times 10^7 \text{ min}^{-1}$ . According to the master-plots method, it was found that the first stage followed the fourth-order (F4) model, while the second stage was described by the second-order (F2) model. Based on the statistical evaluation, the devolatilization behaviors reconstructed from overall kinetic expression agree reasonably well with the experimental data, proving its practical importance for designing a pyrolytic processing system using anaerobic sewage sludge as raw material. This study contributes by providing useful insights that can be applied to a large-scale biorefinery as a critical step towards producing biofuels coupled to municipal wastewater treatment in an environmentally sustainable manner.

---

José Luiz Francisco Alves and Constantino Gomes da Silva contributed equally to this work and shared senior authorship.

---

**Highlights** A new option for useful biorefinery products from municipal wastewater treatment

High-ash anaerobic sewage sludge is an underutilized feedstock for pyrolysis

Bioenergy potential of high-ash anaerobic sewage sludge via pyrolysis was evaluated

New data for optimizing a pyrolysis process in an integrated biorefinery approach

The pyrolysis can be combined with anaerobic digestion for sustainable biorefining

---

✉ José Luiz Francisco Alves  
zeluiz\_alves@hotmail.com; jose.alves@posgrad.ufsc.br

<sup>2</sup> Institute of Geosciences and Engineering, Federal University of Southern and Southeastern of Pará, Marabá, Pará 68507-590, Brazil

<sup>1</sup> Graduate Program in Chemical Engineering, Department of Chemical Engineering and Food Engineering, Federal University of Santa Catarina, Florianópolis, Santa Catarina 88040-900, Brazil

<sup>3</sup> Department of Engineering, Federal University of Technology – Paraná (UTFPR) Francisco Beltrão, Paraná 85601-970, Brazil

**Keywords** Sewage sludge · Bioenergy potential · Pyrolysis kinetics · Thermodynamic evaluation · Sustainable biorefinery

## 1 Introduction

The development and implementation of new integrated biorefinery systems (for converting organic wastes into bioenergy or biofuels) can provide new renewable energy sources, minimizing the effect of greenhouse gas emissions and diversifying the global energy matrix. Biowastes are promising candidates for conversion into carbon-neutral bioenergy by using biological or thermochemical processes. The valorization of abundant biowastes with bioenergy conversion technologies can contribute to sustainable development, bioresource diversity, and environmental benefits. Thus, the biowaste-based biorefinery concept can play an essential role in the upcoming circular-bioeconomy with future perspectives for biowaste exploitation in bioenergy industries with a self-sustainable scenario [1]. Brazil presents a significant deficit in primary sanitation services. According to the Brazilian Secretary of Environment Sanitation [2], 4.2 billion m<sup>3</sup> in sanitary sewage was treated in 2017, which corresponds to just 46% of the municipal sewage generated. Anaerobic digestion is suitable for converting complex organic feedstocks into energy-rich biogas (bioenergy production) with the potential for both bioremediation and waste stabilization [3].

The use of up-flow anaerobic sludge blanket (UASB) reactors offers an eco-friendly option for sewage treatment by anaerobic digestion with significant biogas production from the decomposition of organic matter [4, 5]. The use of a UASB configuration is well established in Brazil for municipal sewage treatment due to favorable climatic conditions (for example, the ambient temperature usually above 20 °C) and lower implementation costs [6, 7]. The operation of UASB reactors in Brazil produces a large amount of solid waste known as “anaerobic sewage sludge,” which contains pollutants including a high level of pathogens, toxic components, heavy metals, persistent organic pollutants, and unwanted nutrient content, with an average production rate estimated at 16 gSTS hab<sup>-1</sup> day<sup>-1</sup> [8, 9]. Traditional final disposal options for municipal sewage sludge include landfilling and agriculture; however, these applications are discouraged by strict environmental restrictions [10, 11]. In addition, disposal in Brazilian landfills is costly, estimated at US\$ 70 per ton [12]. The biorefinery concept based on the combination of biochemical and thermochemical conversion has recently received substantial attention for its potential to turn organic waste into bioenergy, resulting in progressive replacement of fossil fuels [13, 14]. Thus, bioenergy recovery from anaerobic sewage sludge can decrease operating costs in municipal wastewater treatment and convert its organic fraction into bioenergy.

Pyrolysis can serve as a practical step for the valorization of this underutilized feedstock, providing volume reduction, sterilization, and destruction of organic contaminants, while producing value-added biofuels such as biochar, bio-oil, and bio-syngas [10]. Compared with incineration and gasification, sewage sludge pyrolysis can be an energetically self-sufficient thermal route for bioenergy recovery with low and acceptable gas emissions, zero waste generation, and compact equipment [9]. There are presently few commercial-scale pyrolysis-based plants for sewage sludge processing due to the complexity of the adequate design of pyrolysis equipment, which creates a significant barrier to conducting pyrolysis [9]. Thus, the potential to convert high-ash anaerobic sewage sludge to bioenergy via pyrolysis remains underutilized. Proper knowledge about pyrolysis kinetics and process thermodynamics is crucial to maturing this technology at a commercial scale and providing input data relevant to the successful design and scale-up of pyrolytic systems [15, 16]. There is little reporting in the literature on the determination of the kinetic and thermodynamic parameters for high-ash sewage sludge pyrolysis [16].

Thermogravimetric analysis (TGA) is a fundamental source of information about gas–solid decomposition reactions (to understand the behavior of complex conversion processes) such as pyrolysis, which can be useful for identifying pyrolysis conditions in pilot-scale facilities [17, 18]. Non-isothermal thermogravimetric data can be applied to determine the kinetic triplet (activation energy ( $E_a$ ), frequency factor ( $A$ ), and reaction model ( $f(\alpha)$ )) and thermodynamic parameters (Gibbs free energy ( $\Delta G$ ), enthalpy ( $\Delta H$ ), and entropy ( $\Delta S$ )) [1, 15, 19]. The knowledge of these parameters is useful for prediction and simulation of the complex thermal decomposition process, to calculate energy balances, and to ascertain the feasibility of the pyrolytic conversion of organic wastes [15, 19, 20].

To the best of our knowledge, there is a lack of updated information about kinetic and thermodynamic data about pyrolysis of high-ash anaerobic sewage sludge that can support the design and optimization of adequate commercial-scale pyrolysis facilities, within a biorefinery context. Still, most studies found in related literature give insight into the kinetic and thermodynamic information based on the single-step approach to derive the kinetic parameters [16, 21] and scarcely attempted to verify their resulting kinetic parameters by simulating or reconstructing the non-isothermal experimental behavior. In parallel, there is a difficulty in reliable estimation of kinetic triplet and thermodynamic parameters derived from pyrolysis of complex organic solid (like sewage sludge) due to its heterogeneous composition [22, 23]. Thus, it is expected that the pyrolytic conversion of sewage sludge to bioenergy

products can occur as a sequence of reaction stages [24]. In this way, special attention was given to pyrolysis characteristics, where a multi-step kinetic approach was adopted in accordance with newly published recommendations of the ICTAC Kinetics Committee [25].

A new option for the development of valuable biorefinery products emphasizes the integration of biochemical conversion (anaerobic digestion of organic matter into biogas) and subsequent thermochemical processing (pyrolytic conversion of anaerobically digested organic matter to biofuels). The original contribution of this study is that it introduces the possibility of creating a new efficient integrated platform for sustainable municipal wastewater treatment linked with bioenergy production by integrating anaerobic digestion and pyrolysis. The study conducted a detailed investigation of the kinetic triplet and thermodynamic parameters of pyrolysis of high-ash anaerobic sewage sludge to assess its bioenergy potential, and provide reliable inputs for the design of optimum reactors for pyrolysis conditions. For this purpose, four different isoconversional methods, the compensation effect factor method, and the master plots method are used to deduce a suitable kinetic triplet, which can describe each step involved in pyrolytic conversion process, given the lack of information about this approach in the literature. In addition, basic physicochemical properties were determined to support the design of a thermal conversion processing plant. This study can support the implementation of a commercial-scale biorefinery system to produce valuable biofuels coupled to municipal wastewater treatment.

## 2 Materials and methods

### 2.1 Feedstock harvesting, preparation, and characterization procedures

A high-ash anaerobic sewage sludge sample was collected from a municipal anaerobic wastewater treatment plant belonging to the Paraná Sanitation Company (SANEPAR), located in Curitiba city (Southern Brazil) [22]. The Sanepar Company uses an established technology for municipal wastewater treatment, which involves preliminary treatment and anaerobic digestion, in the following steps and equipment (emphasizing the sludge line): (1) mechanical screening to separate large solids, (2) passage through a grit chamber to remove settleable matter such as sand and other inorganic particles, (3) passage to a UASB reactor with hydraulic retention time of 6–10 h to anaerobically digest the organic matter, (4) a centrifuge system for dewatering the high-ash anaerobic sewage sludge, and (5) a hygienization system to destroy pathogens present in high-ash anaerobic sewage sludge. The sample studied was collected after hygienization; it was dried until attaining residual moisture between 10 and 20% using a rotary

granulator dryer (Bruthus model, Albrecht, Brazil) at a steady temperature of 473 K.

The proximate analysis was carried out in a thermogravimetric analyzer model DTG-60 (Shimadzu, Kyoto, Japan), according to the ASTM E-1131 [15] standard method. The ultimate analysis was performed using the following standards: the composition, in weight, of carbon (C), hydrogen (H), and nitrogen (N) was obtained using an Elemental Analyzer 2400 CHN Series II (Perkin-Elmer, Shelton, United States); the sulfur (S) content was measured using inductively coupled plasma optical emission spectrometry (ICP-OES Analyzer, Spectro Arcos, Mahwah, United States); the chlorine (Cl) content was measured using the Schöniger Method; and the oxygen (O) content was determined by difference on a dry basis [11]. The higher heating value (HHV) was measured using a bomb calorimeter model C200 (IKA, Wilmington, USA) following the ASTM D5865 standard. The lower heating value (LHV) was calculated with the following equation:  $LHV (MJ kg^{-1}) = HHV (MJ kg^{-1}) - 0.2183 H (\%)$  [15]. Previous characterization of anaerobic sewage sludge can be found in Languer et al. [22].

### 2.2 Thermogravimetric analysis

A thermogravimetric analyzer model DTG-60 (Shimadzu, Kyoto, Japan) with an accuracy of weight loss of 0.1  $\mu g$  was employed to study the pyrolysis characteristics of the high-ash anaerobic sewage sludge. In each non-isothermal experimental run, about 10 mg of the sample was loaded into a platinum crucible. Initially, a gas purge process with oxygen-free nitrogen was performed (purity up to 99.996%) for 60 min to effectively remove the atmospheric air in the oven before the pyrolysis tests. Next, a constant heating rate of 10, 25, 50, and 90  $K min^{-1}$  was applied to heat the sample up to 1225 K at atmospheric pressure. Nitrogen gas was supplied at a flow rate of 100  $mL min^{-1}$  to ensure an inert atmosphere for the experiment. To minimize mass and heat transfer limitations in the course of thermal degradation, the particle size of the high-ash anaerobic sewage sludge is in the order of 106  $\mu m$  (< 140 mesh). Three repetitions under the given conditions were carried out to ascertain the thermogravimetric quality and the satisfactory reproducibility of experimental results.

### 2.3 Mathematical modeling to obtain the kinetic triplet

#### 2.3.1 Determination of the activation energy ( $E_a$ )

The kinetic triplet of high-ash anaerobic sewage sludge was determined based on thermogravimetric data using four different isoconversional methods, the compensation effect factor method, and the master plots method. The pyrolysis process is based on the solid-volatiles conversion, and therefore,

the thermal decomposition process rate can be described by a fundamental expression (Eq. (1)).

$$\frac{d\alpha}{dt} = k(T)f(\alpha) = Ae^{-\frac{E_a}{RT}}f(\alpha) \quad (1)$$

where  $k(T)$  represents the rate constant of the reaction that is dependent on temperature ( $T$ ),  $\alpha$  is the degree of conversion,  $f(\alpha)$  represents the reaction model (conversion function),  $A$  represents the frequency (pre-exponential) factor ( $\text{min}^{-1}$ ),  $E_a$  ( $\text{J mol}^{-1}$ ) represents the activation energy, and  $R$  represents the universal gas constant ( $8.314 \text{ J K}^{-1} \text{ mol}^{-1}$ ).

For non-isothermal thermogravimetric analysis conducted at different heating rates, the introduction of the heating rate ( $dT/dt = \beta$ ,  $\text{K min}^{-1}$ ) in the fundamental expression leads to the following equation (Eq. (2)):

$$\frac{d\alpha}{dT} = \frac{A}{\beta} e^{-E_a/RT} f(\alpha) \quad (2)$$

The integration of Eq. (2) with constant heating rate conditions results in

$$g(\alpha) \equiv \int_0^\alpha \frac{d\alpha}{f(\alpha)} = \frac{A}{\beta} \int_{T_0}^T e^{-E_a/RT} dT \quad (3)$$

The integral equation (Eq. (3)) above does not have an analytical resolution, and therefore, isoconversional methods such as Flynn–Wall–Ozawa (FWO), Kissinger–Akahira–Sunose (KAS), and Starink (STK) are useful tools for estimating the activation energy. The isoconversional analysis does not require initial knowledge of reaction models and the pre-exponential factor; thus, the apparent activation energy is determined as a function of conversion [15, 17].

### 2.3.2 The Flynn–Wall–Ozawa method

Mathematical resolution by the FWO integral isoconversional method is based on the Doyle approximation equation and can be expressed by Eq. (4) [17]:

$$\log \beta = \log \left( \frac{A_a E_a}{R g(\alpha)} \right) - 2.315 - 0.4567 \frac{E_a}{RT} \quad (4)$$

The plot of  $\log \beta$  ( $y$ -axis) versus  $1/T$  ( $x$ -axis) at a selected conversion ( $\alpha$ ) was used to calculate the activation energy ( $E_a$ ) from the plot slope ( $-0.4567E_a/R$ ).

### 2.3.3 Kissinger–Akahira–Sunose method

The integral isoconversional method proposed by KAS involves an approximation using the Murray and White equation that can be described as Eq. (5) [17]:

$$\ln \left( \frac{\beta}{T^2} \right) = \ln \left( \frac{AR}{E_a g(\alpha)} \right) - \frac{E_a}{RT} \quad (5)$$

The slope ( $-E_a/R$ ) of the straight line plotted by  $\ln(\beta/T^2)$  ( $y$ -axis) versus  $1/T$  ( $x$ -axis) at a constant value of conversion ( $\alpha$ ) can provide the value of the activation energy ( $E_a$ ).

### 2.3.4 Starink method

Another integral isoconversional method originates from the Starink approximation equation and can be expressed as follows [17]:

$$\ln \left( \frac{\beta}{T^{1.92}} \right) = -1.0008 \left( \frac{E_a}{RT} \right) + \text{Constant} \quad (6)$$

Assuming the conversion ( $\alpha$ ) in Eq. (6) has a fixed value, the activation energy ( $E_a$ ) can be calculated from the slope ( $-1.0008E_a/R$ ) of the straight line obtained by plotting  $\ln(\beta/T^{1.92})$  ( $y$ -axis) versus  $1/T$  ( $x$ -axis).

### 2.3.5 Determination of the frequency factor ( $A$ )

The frequency factor was determined from a linear relationship between the activation energy and the pre-exponential factor, known as the compensation effect method (Eq. (7)) [17].

$$\ln(A) = aE_a + b \quad (7)$$

In Eq. 7,  $a$  and  $b$  are compensation parameters dependent on the heating rate and are attained using linear regression for different reaction models. For this purpose, a model-fitting method is applied to a single-heating rate run. By substituting different models into the rate equation (Eq. 2) and fitting it to experimental data, different pairs of the Arrhenius parameters ( $\ln A_i$  and  $E_{a,i}$ ) can be obtained [17]. The  $A$  values are then obtained from  $E_a$  values previously calculated from an isoconversional method.

### 2.3.6 Determination of the reaction model ( $f(\alpha)$ )

The master plot based on the integral form of the kinetic data (Eq. (8)) is a method commonly used for estimation of the reaction model in a heterogeneous reaction. The method consists of plotting theoretical curves (based on reaction model equations found in the literature) and experimental data, with the relationship presented in Eq. (8). The experimental data that best fits the theoretical curve indicates the reaction model.

$$\frac{g(\alpha)}{g(0.5)} = \frac{p(x)}{p(x_{0.5})} \quad (8)$$



In Eq. (8) parameter  $p(x)$  is the integral form of the reaction model and an approximation for the temperature integral equation with  $x = E_a/RT$  and term 0.5 represents the value when the conversion reaches the conversion of 50%. The expression  $p(x)$  can be calculated by the Senum–Yang approximation. The reaction model used to describe solid-state reaction kinetics is reported in our previous study and includes the power-law (P2, P3, P4, and P2/3), Avrami–Erofeev (A2, A3, and A4),  $n$ -order reaction (F1, F2, F3, and Fn), geometrical contraction (R2 and R3), and diffusion (D1, D2, D3, and D4) [26].

## 2.4 Thermodynamic parameters

The thermodynamic parameters reflect the nature of a thermal process, which involves simultaneous and secondary reactions. These parameters are crucial for optimizing and adjusting the pyrolytic conversion of high-ash anaerobic sewage sludge. The standard equations used to calculate the thermodynamic parameters, which include changes in Gibbs free energy ( $\Delta G$ ) (Eq. 9), enthalpy ( $\Delta H$ ) (Eq. 10), and entropy ( $\Delta S$ ) (Eq. 11), were based on activated complex theory [15].

$$\Delta G = E_a + RT_m \ln \left( \frac{k_B T_m}{hA} \right) \quad (9)$$

$$\Delta H = E_a - RT \quad (10)$$

$$\Delta S = \frac{\Delta H - \Delta G}{T_m} \quad (11)$$

where  $k_B$ ,  $h$ , and  $T_m$  are the Boltzmann constant ( $1.381 \times 10^{-23} \text{ J K}^{-1}$ ), the Plank constant ( $6.626 \times 10^{-34} \text{ J s}^{-1}$ ), and the maximum temperature peak achieved from the differential thermogravimetric data, respectively.

## 3 Results and discussion

### 3.1 Characteristics of the high-ash anaerobic sewage sludge

Table 1 summarizes the main physicochemical characteristics for high-ash anaerobic sewage sludge compared with representative low-rank coals. The characteristics obtained for high-ash anaerobic sewage sludge are in conformity with other sewage sludge samples found in the literature [16, 29, 30]. The moisture content of anaerobic sewage sludge was 8.70 wt%, on a received basis. This value fell within the acceptable value of moisture for thermochemical biomass conversion, which is below 10 wt% [31].

The moderate volatile matter (53.93 wt%) and lower fixed carbon (3.09 wt%) contents can favor the yield of volatile

products, i.e., bio-oil and pyrolytic syngas, produced using fast pyrolysis from condensation [30]. The high-ash anaerobic sewage sludge sample is characterized by higher ash content (~43 wt%) than traditional biomass feedstocks, which can cause practical difficulties for thermal processing of this biowaste. Various practices can be used to avoid slagging problems during thermal processing, including an optimal temperature for thermal conversion, preliminary pretreatment, or application of useful additives [15]. The results found for proximate analysis had an order of magnitude in the medium range reported for lignite coal and biomass [10].

The primary individual elements found in high-ash anaerobic sewage sludge were carbon, oxygen, and hydrogen with contents of 23.66 wt%, 21.42 wt%, and 4.95 wt% on a dry basis, respectively. These carbon, hydrogen, and oxygen contents are lower than found in the elemental analysis of typical lignocellulosic residues [10]. The nitrogen (3.15 wt%) and sulfur (3.44 wt%) contents are higher than those typically found in biomass-based [10]. This can contribute to possible emissions of toxic and corrosive gases, such as nitrogen oxides ( $\text{NO}_x$ ) and sulfur oxides ( $\text{SO}_x$ ), from the thermochemical conversion of high-ash anaerobic sewage sludge. The HHV of high-ash anaerobic sewage sludge was shown to be  $14.00 \text{ MJ kg}^{-1}$ , which is similar to values reported for low-rank fuels, including subbituminous and lignite coals [27, 28]. In summary, the feedstock analyzed is abundant and promising for bioenergy purposes in Brazil. In addition, the characteristics found indicate that high-ash anaerobic sewage sludge has the potential to compete with low-rank coals [10, 27, 28].

### 3.2 Thermal decomposition analysis

Figure 1 shows the TG/DTG curves for dried high-ash anaerobic sewage sludge as a function of temperature at a heating rate of 10, 25, 50, and  $90 \text{ K min}^{-1}$ .

The pyrolytic behavior of high-ash anaerobic sewage sludge can be divided into main three-reaction zones, as follows: dehydration at  $< 398 \text{ K}$  (drying zone), devolatilization between 398 and 953 K (active pyrolysis zone), and decomposition of char and inorganic non-combustible material at  $> 953 \text{ K}$  (passive pyrolysis zone).

The first zone is related to water evaporation and the decomposition of light extractives. In Table 2, the weight loss percentages (dry basis) in each devolatilization stage and the final temperature are shown for the pyrolysis of high-ash anaerobic sewage sludge. An average mass loss of 54.19 wt% was observed at 1223 K (pyrolysis ending temperature), which was close to 53.93 wt% of volatile matter in proximate analysis). The mass-loss rate was highest at the range of 398–953 K (47.56 wt% on a dry basis). The active pyrolysis zone shows two partially overlapping stages of mass loss. The first devolatilization stage with an average mass loss of 27.80 wt%

**Table 1** Proximate analysis, ultimate analysis, and heating values (HHV and LHV) for anaerobic sewage sludge and low-rank coals found in literature

Sample	Anaerobic sewage sludge <sup>a</sup>	Subbituminous coal <sup>b</sup>	Lignite coal <sup>c</sup>
Proximate analysis (wt.%, dry basis)			
Volatile matter	53.93	24.70	38.04
Fixed carbon	3.09	29.80	12.75
Ash	42.98	45.50	49.21
Ultimate analysis (wt.%, dry basis)			
Carbon	23.66	37.40	30.97
Hydrogen	4.95	3.80	2.69
Nitrogen	3.15	0.70	4.82
Sulfur	3.44	2.70	1.69
Chlorine	0.40	–	–
Oxygen	21.42	9.90	10.62
Heating value (MJ kg <sup>-1</sup> , dry basis)			
HHV	14.00	15.23	9.99
LHV	13.00	14.27	–

<sup>a</sup>This work. Note that these results were previously published in Languer et al. [22]

<sup>b</sup>Domenico et al. [27]

<sup>c</sup>Uyar and Suyadal [28]

corresponded to the range of 398 K to 717 K, which occurs due to the presence of reactive organic components (biodegradable organic material) at low pyrolysis temperature. The second devolatilization stage (647–953 K) corresponded to an average mass loss of 19.77 wt% and can be attributed to the pyrolysis of less reactive organic components (mainly bacterial matter) at lower pyrolysis temperatures [23]. The passive pyrolysis zone is linked to slow thermal decomposition of char and inorganic materials such as calcium carbonate [16, 23]. The devolatilization stage (active pyrolysis zone) was defined for kinetic and thermodynamic analysis, as also established by Alves et al. [26].

### 3.3 Kinetic triplet examination

#### 3.3.1 Isoconversional methods results

Figure 2a shows the straight-line plotted using the Flynn–Wall–Ozawa (FWO), Kissinger–Akahira–Sunose (KAS), and Starink methods at the conversion range of  $0.1 \leq \alpha \leq 0.9$  for each stage in the active pyrolysis zone.

In Stage I, a large gap is seen between the straight lines for the conversion of 0.1 and 0.2 with a different slope of the straight line for conversion 0.1 for all isoconversional methods used. This gap is associated to a slow conversion rate

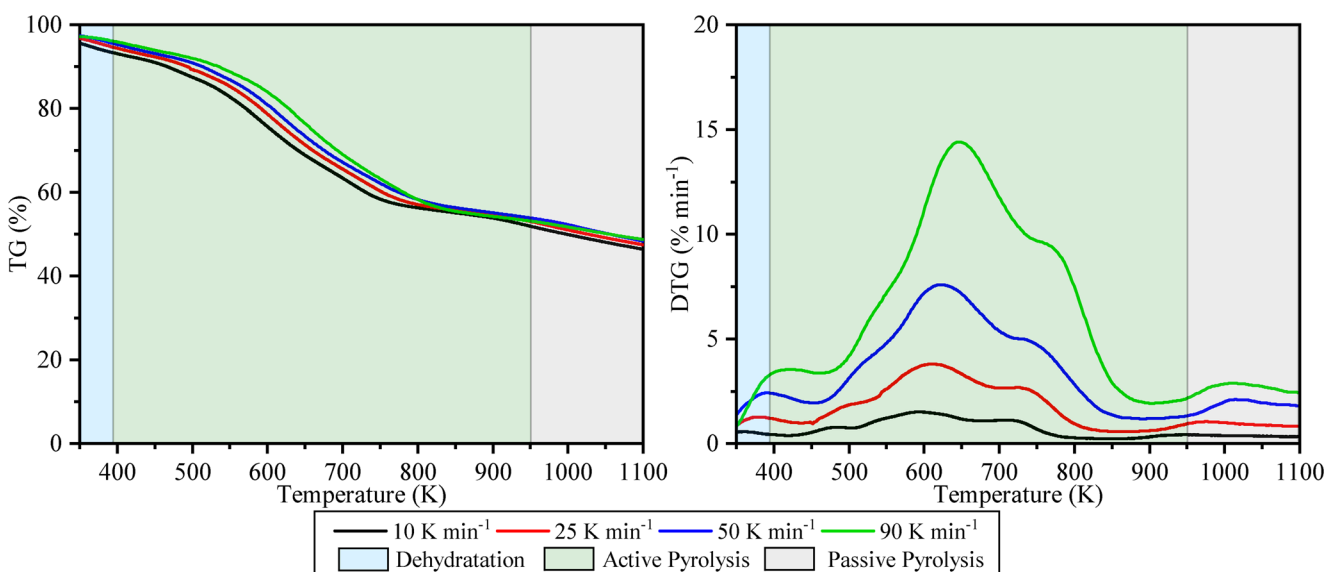


**Fig. 1** Overlap of TG and DTG curves of dried high-ash anaerobic sewage sludge pyrolysis under heating rates of 10, 25, 50, and 90 K min<sup>-1</sup>

**Table 2** TG-DTG characteristics of anaerobic sewage sludge at heating rates of 10, 25, 50, and 90 K min<sup>-1</sup>

$\beta$ (K min <sup>-1</sup> )	Active pyrolysis zone						Passive pyrolysis zone		
	Stage I			Stage II			$T_i$ (K)	$T_f$ (K)	Mass loss (%) <sup>a</sup>
	$T_i$ (K)	$T_f$ (K)	Mass loss (%) <sup>a</sup>	$T_i$ (K)	$T_f$ (K)	Mass loss (%) <sup>a</sup>			
10	398	647	25.69	647	823	19.18	823	1223	16.33
25	398	665	26.53	665	848	19.54	848	1223	14.62
50	398	683	28.66	683	903	19.70	903	1223	13.23
90	398	717	30.30	717	953	20.65	953	1223	9.27
Average mass loss (%)	-	-	27.80	-	-	19.77	-	-	13.36

<sup>a</sup>Dry basis

in the active pyrolysis zone; i.e., an increase in 10% of conversion requires a considerable increase of temperature at the beginning of pyrolysis in Stage I. The different slope for 0.1 demonstrates that high energy (Table 3) is required to generate an activated complex and break down the chemical bonds at low temperatures. This large gap is characteristic of biomass pyrolysis in initial conditions of devolatilization (typically, conversions below 0.2 and low temperatures) and can easily

be identified in previously published studies [32–35]. The determination coefficient ( $R^2$ ) values below 0.9 ( $R^2 = 0.8023–0.8150$ ) observed in Table 3 indicate a greater dispersion of the initial conversion data. The approximation of the straight lines for the conversions of 0.3 and 0.9 is observed along the evolution of the conversion. This behavior indicates a gradual change (from 97.71–100.93 kJ mol<sup>-1</sup> to 113.73–117.26 kJ mol<sup>-1</sup>) in the energy required to break the chemical

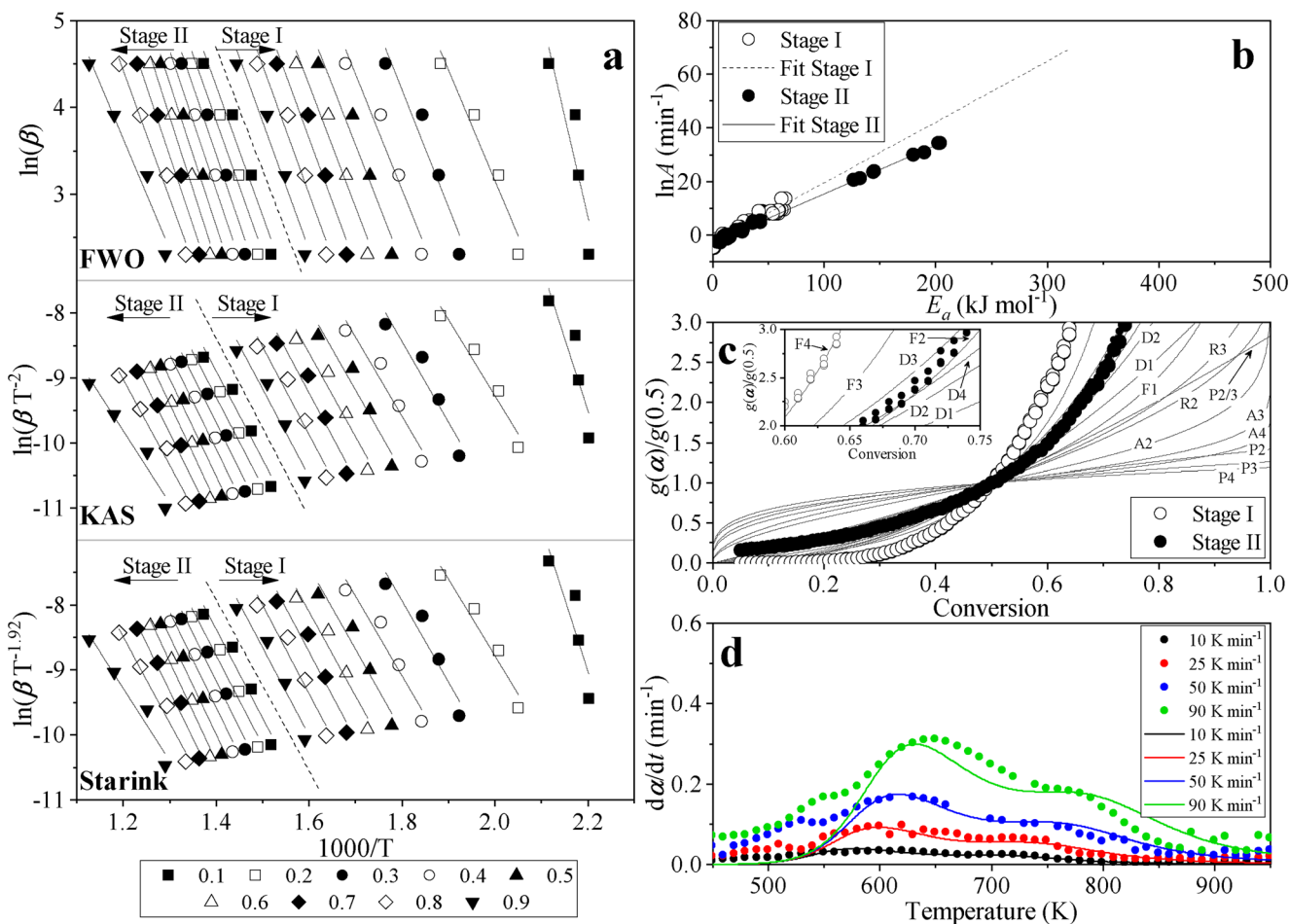


**Fig. 2** **a** The linear fit curves obtained from the FWO, KAS, and STK methods, **b** the linear fitted curves for the compensation effect, **c** master plot curves, and **d** predicted (line) and experimental (symbol)  $d\alpha/dt$  vs.  $T$

**Table 3** Kinetic and Thermodynamic parameter estimated for each stage in the active pyrolysis zone of dried anaerobic sewage sludge

Conversion	Kinetic						Thermodynamic			
	FWO		KAS		Starink		$\Delta H$ (kJ mol <sup>-1</sup> )	$\Delta G$ (kJ mol <sup>-1</sup> )	$\Delta S$ (J mol <sup>-1</sup> )	
	$E_a$ (kJ mol <sup>-1</sup> )	$R^2$	$E_a$ (kJ mol <sup>-1</sup> )	$R^2$	$E_a$ (kJ mol <sup>-1</sup> )	$R^2$				
Stage I	0.1	183.34	0.8023	185.16	0.8028	185.62	0.8150	110.37	157.43	-101.98
	0.2	100.93	0.9424	97.71	0.9428	98.13	0.9512	109.99	162.10	-102.76
	0.3	106.94	0.9192	103.47	0.9197	103.91	0.9313	109.72	165.51	-103.28
	0.4	105.28	0.9390	101.29	0.9395	101.75	0.9490	109.50	168.23	-103.68
	0.5	108.84	0.9387	104.69	0.9391	105.17	0.9487	109.33	170.35	-103.97
	0.6	111.48	0.9383	107.18	0.9388	107.67	0.9485	109.18	172.21	-104.22
	0.7	115.89	0.9472	111.54	0.9476	112.04	0.9559	109.04	173.95	-104.45
	0.8	117.20	0.9517	112.64	0.9520	113.16	0.9598	108.90	175.76	-104.68
	0.9	117.01	0.9477	112.12	0.9481	112.65	0.9567	108.75	177.68	-104.91
	Average <sup>a</sup>	117.26	0.9195	113.73	0.9199	114.21	0.9292	109.42	169.24	-103.77
Stage II	0.1	118.52	0.9496	113.16	0.9500	113.71	0.9586	110.60	208.70	-142.16
	0.2	120.18	0.9492	114.69	0.9496	115.25	0.9584	110.49	210.57	-142.31
	0.3	125.61	0.9603	120.20	0.9606	120.77	0.9674	110.38	212.40	-142.47
	0.4	127.13	0.9615	121.57	0.9618	122.16	0.9684	110.27	214.29	-142.62
	0.5	130.26	0.9728	124.67	0.9730	125.27	0.9777	110.16	216.18	-142.77
	0.6	132.33	0.9753	126.63	0.9755	127.24	0.9798	110.05	218.07	-142.91
	0.7	127.55	0.9753	121.34	0.9756	121.95	0.9801	109.92	220.33	-143.09
	0.8	116.82	0.9736	109.72	0.9738	110.33	0.9792	109.75	223.34	-143.31
	0.9	100.90	0.9516	92.37	0.9522	92.99	0.9636	109.46	228.29	-143.66
	Average <sup>a</sup>	121.87	0.9616	115.75	0.9619	116.34	0.9690	110.12	216.95	-142.81

<sup>a</sup> Average calculated using the data for all conversion range (variation of 0.001)

bonds, while at conversions greater than 0.7 constant values of activated energy are observed (Table 3). The average values of  $E_a$  for Stage I were 117.26 kJ mol<sup>-1</sup> for the FWO method, 113.73 kJ mol<sup>-1</sup> for the KAS method, and 114.21 kJ mol<sup>-1</sup> for the Starink method. Unlike Stage I, Stage II is characterized by a nearly parallel and straight line through most of the conversion range (between conversions of 0.1 and 0.8). The nearly straight lines initially indicate that the conversion occurs quickly when compared with Stage I, in which the increase of 10% of conversion occurs over a short temperature range at a conversion range of 0.1 and 0.8. In addition, straight lines can also indicate that the decomposition reaction occurs under sufficient reaction energy. At this stage, the  $E_a$  value starts near the end of that observed for Stage I (113.16–118.52 kJ mol<sup>-1</sup>), where a gradual increase is observed with conversion until it reaches 0.6 (126.63–132.33 kJ mol<sup>-1</sup>), followed by a subsequent energy reduction of  $E_a$ , as shown in Table 3. The average values of  $E_a$  for Stage I were 121.87 kJ mol<sup>-1</sup> for the FWO method, 115.75 kJ mol<sup>-1</sup> for the KAS method, and 116.34 kJ mol<sup>-1</sup> for Starink method.

Stage I and Stage II had a similar average value of  $E_a$ , which indicates that in the active pyrolysis zone of dried anaerobic sewage sludge the process occurs stably, with an

approximately constant value of activation energy. Both stages of pyrolysis of dried anaerobic sewage sludge showed lower  $E_a$  value than sorghum straw (132.03 kJ mol<sup>-1</sup>) [20], pine-fruit shell (178.78–394.99 kJ mol<sup>-1</sup>) [26], sub-bituminous coal (277.3–287.4 kJ mol<sup>-1</sup>) [36], canola residue (194.3 kJ mol<sup>-1</sup>) [37], castor residue (167.1 kJ mol<sup>-1</sup>) [37], carrot grass (267 kJ mol<sup>-1</sup>) [32], and Wolffia biomass (136–172 kJ mol<sup>-1</sup>) [33] (all under slow pyrolytic conditions).

### 3.3.2 Pre-exponential factor determination

Figure 2b presents the linear plot obtained by the compensation effect for the pyrolysis of each stage in the active pyrolysis zone of anaerobic sewage sludge. The predictions from this method had high determination coefficients (for Stage I  $R^2 = 0.9315$ , and for Stage II  $R^2 = 0.9977$ ) with compensation parameters of  $a = 0.2267$  and  $b = -3.1700$  for Stage I and  $a = 0.1823$  and  $b = -2.9100$  for Stage II. The lower adjustment for Stage I indicates a higher dispersion of the experimental data, which is associated with the possible occurrence of multiple and complex reactions during the feedstock devolatilization in this stage [17]. The pre-exponential factors for the first stage and second stage are respectively  $7.39 \times 10^9$  and  $8.80 \times 10^7$



$\text{min}^{-1}$ , which are lower than the orders of magnitude related to the other feedstocks suggested for pyrolysis such as reed macroalgae ( $10^{12}$ – $10^{16} \text{ min}^{-1}$ ) [15], pine-fruit shell ( $10^{16}$ – $10^{24} \text{ min}^{-1}$ ) [26], plastic waste ( $10^{20}$ – $10^{25} \text{ min}^{-1}$ ) [34], rice husk ( $10^{14}$ – $10^{15} \text{ min}^{-1}$ ) [38], pine wood ( $10^{14}$ – $10^{15} \text{ min}^{-1}$ ) [38], and bamboo ( $10^{13}$ – $10^{15} \text{ min}^{-1}$ ) [38]. The lower value of pre-exponential factors in the anaerobic sewage sludge indicates a tendency to obtain a favorable pyrolytic decomposition, and that it can be a commercially viable feedstock. Since the probability that molecules will collide in a proper molecular orientation is higher, a lower rate of molecular collisions and less reaction energy is required to initiate the thermal conversion [19, 37].

### 3.3.3 Reaction model evaluation

In Fig. 2c, the experimental master plot curves for Stage I and Stage II indicate that the reaction models most adequate for describing the pyrolysis of these stages are fourth-order ( $F4 = (1 - \alpha)^4$ ) and second-order ( $F2 = (1 - \alpha)^2$ ) reaction models, respectively. The  $n$ -order reaction mechanism was also noted in the pyrolysis of sub-bituminous coal [36]. The thermal decomposition rate corresponds to the concentration of reactant raised to a specific power “ $n$ ” in an  $n$ -order reaction model [15]. According to master plot results, in the active pyrolysis zone of anaerobic sewage sludge there is a mechanism change from a fourth-order reaction model at lower temperatures (398–673 K) to a second-order reaction model at higher temperatures (673–973 K). The determination of a suitable reaction model is fundamental to obtaining a better understanding of the complex solid-state reaction mechanisms due to the presence of different organic compounds in anaerobic sewage sludge.

### 3.3.4 Verification of the kinetic triplet

The thermal behavior of the active pyrolysis zone of high-ash anaerobic sewage sludge was simulated (Fig. 2d) using the kinetic parameter data estimated by the isoconversional method of Starink, the compensation effect, the master plot, Eq. (2), and the Runge–Kutta 4th numerical method. Equation (12) describes the pyrolysis process mathematically.

$$\left(\frac{d\alpha}{dt}\right) = \eta_{\text{Stage I}} (7.39 \times 10^9) e^{114210/RT} (1-\alpha)^4 + \eta_{\text{Stage II}} (8.80 \times 10^7) e^{116340/RT} (1-\alpha)^2 \quad (12)$$

In Eq. (12), parameter  $\eta$  is the conversion fraction for each stage in the active pyrolysis zone and was 0.56 and 0.20 for Stage I and Stage II, respectively. Figure 2d indicates that the kinetic parameters estimated from the isoconversional

methods, compensation effect, and master plot can provide a satisfactory thermal behavior curve. For the temperature range 585–910 K, it is noted that Eq. (12) provides a more suitable fit than the experimental data and has a better fit for heating rates below  $90 \text{ K min}^{-1}$ . On the other hand, at temperatures below 585 K, a lower adjustment is observed. This is due to the use of a single-step mechanism method for calculation. Although it is a common method, the results provide better representation for a region with high conversion rates, as also noted by Alves et al. [39]. The  $R^2$  obtained for all temperature ranges calculated (398–973 K) were 0.8285, 0.8207, 0.8519, and 0.8796 for heating rates of 10, 25, 50, and  $90 \text{ K min}^{-1}$ , respectively, while the  $R^2$  for the best fitting range (585–910 K) were 0.9265, 0.9149, 0.9032, and 0.8846 for heating rates of 10, 25, 50, and  $90 \text{ K min}^{-1}$ , respectively. Thus, the results indicate that the kinetic parameters can be satisfactorily applied to thermochemical systems and offer a better reconstruction for the temperature range of 585–910 K, which is a region with the high generation of volatiles. Therefore, the kinetic triplet found is particularly reliable for describing the devolatilization process of high-ash anaerobic sewage sludge by considering the simplicity of the methods.

### 3.4 Thermodynamic aspects

The thermodynamic parameters calculated using the  $E_a$  values obtained from the Starink method are presented in Table 2. The  $\Delta H$  explains the difference of energy between the reagent and the activated complex, i.e., the energy required for dissociation of reagent bonds and formation of reaction products such as gases and biochar. The average  $\Delta H$  values for pyrolysis of anaerobic sewage sludge were  $109.42 \text{ kJ mol}^{-1}$  and  $110.12 \text{ kJ mol}^{-1}$  for Stage I and Stage II, respectively. The positive and low values of  $\Delta H$  suggest a thermodynamically favored endothermic reaction (highly reactive system); thus, less heat energy is required for pyrolysis [19, 40]. The  $\Delta G$  values found were  $169.24 \text{ kJ mol}^{-1}$  and  $216.95 \text{ kJ mol}^{-1}$  for Stage I and Stage II, respectively. These values were higher than the  $\Delta G$  values found for canola residue and castor residue [37], and the value indicates that the pyrolysis of anaerobic sewage sludge requires more available energy than the biomasses cited.

Entropy change ( $\Delta S$ ) is a qualitative measurement of the system reactivity. The values attained were  $-103.77 \text{ J mol}^{-1}$  (for Stage I) and  $-142.81 \text{ J mol}^{-1}$  (for Stage II). Both devolatilization stages showed low reactivity, and consequently, a longer reaction time is necessary to form an activated complex [15]. The negative values in  $\Delta S$  indicate some structural changes needed to achieve a state of thermodynamic equilibrium during the pyrolysis process [16]. Thermodynamic aspects suggest that anaerobic sewage sludge has the potential to compete with newly identified bioenergy

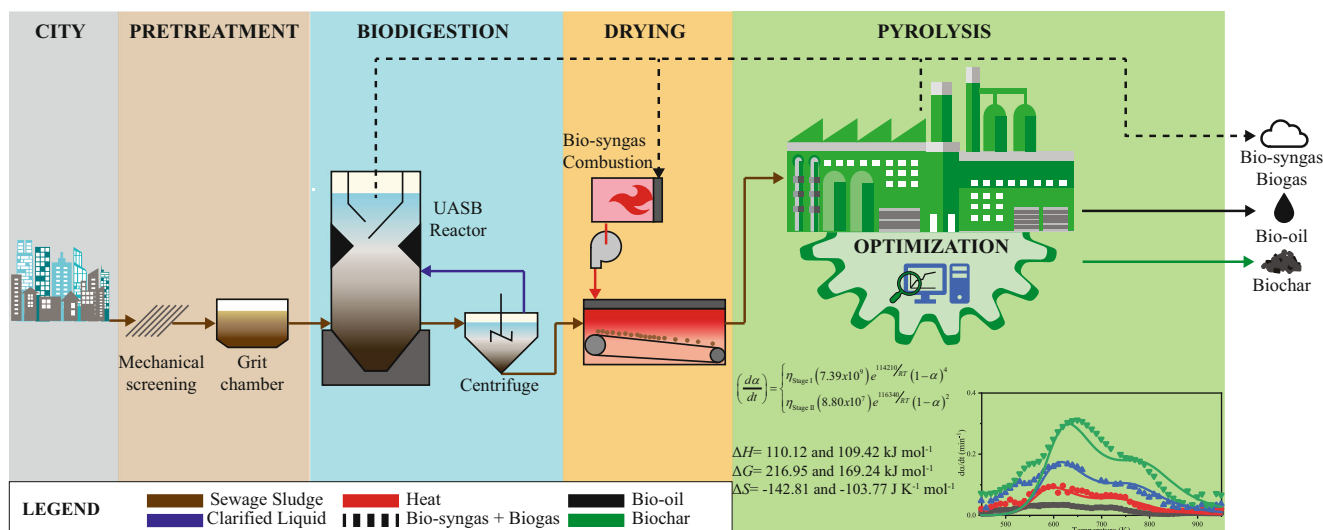


**Fig. 3** Hypothetical scenario of a sustainable biorefinery suggested to produce valuable biofuels coupled to municipal wastewater management

feedstocks [1, 15, 19, 40] and low-rank sub-bituminous coal [36]. These findings suggest that the conversion of anaerobic sewage sludge into energy-rich biofuels using pyrolysis is thermodynamically favorable. Kinetic and thermodynamic parameters are useful inputs for fine-tuning reactor design [1, 40].

### 3.5 Hypothetical biorefinery proposal

Figure 3 presents the schematic scenario of a hypothetical biorefinery suggested to produce valuable biofuels in association with municipal wastewater treatment in a self-sustainable and eco-friendly approach. Recently, the feasibility of similar situations has been proved for bioenergy exploitation from agricultural residues [41] and residual microalgal biomass [1]. The proposed biorefinery scenario is based on the sustainable recovery of bioenergy from municipal wastewater treatment by coupling anaerobic digestion and a pyrolysis process. The municipal sewage is first treated using mechanical screening and a grit chamber, and the pretreated municipal wastewater is anaerobically digested using UASB reactors to produce biogas and anaerobic sewage sludge. The residual sand removed from preliminary sewage treatment can be used as a fine aggregate in concrete for non-structural purposes [12]. The biogas produced by UASB reactors can be converted into heat and electricity in a Combined Heat and Power (CHP) system [14, 41].

For the sludge line, the anaerobic sewage sludge is dewatered using a centrifuge system. The clarified liquid fraction obtained from the centrifuge dewatering is returned to the UASB reactor, while the dewatered sewage sludge can be dried using some of the excess heat generated by the CHP system. The dried anaerobic sewage sludge can be converted into biochar, bio-oil, and bio-syngas using an optimized pyrolysis reactor, which in turn can be designed from the

reliable findings achieved in this study. The bioenergy contained in bio-syngas and bio-oil can be exploited using a CHP system and combustion engine, respectively, to provide the thermal energy required for pyrolytic conversion. The biochar can be used as a soil additive in agriculture. Thus, the use of anaerobic sewage sludge as an alternative green feedstock for pyrolysis can be a promising option for reducing energy costs in municipal wastewater treatment facilities and provides efficient bioenergy recovery with zero-waste generation.

## 4 Conclusions

The possibility to create a new efficient integrated platform for sustainable municipal wastewater treatment by associating it to the creation of useful biorefinery products was identified as a promising and eco-friendly approach. The pyrolysis of high-ash anaerobic sewage sludge valorizes the sludge by converting it to bioenergy products, while providing efficient utilization with zero waste generation, and decreasing operating costs for municipal wastewater treatment. This underutilized feedstock can compete favorably with low-rank fuels. The kinetic and thermodynamic parameters demonstrate that the pyrolysis of high-ash anaerobic sewage sludge holds high potential for creating valuable biorefinery products. The results presented here create new options for optimizing municipal wastewater treatment by associating it to the creation of bioenergy products.

**Funding** This work was supported by the Brazil's National Council for Scientific and Technological Development (CNPq/Brazil Process 458412/2014-7 and 303742/2017-8) and the Coordination for the Improvement of Higher Education Personnel (CAPES/Brazil Finance Code 001).

## References

- Shahid A, Ishfaq M, Ahmad MS, Malik S, Farooq M, Hui Z, Batawi AH, Shafi ME, Aloqbi AA, Gull M, Mehmood MA (2019) Bioenergy potential of the residual microalgal biomass produced in city wastewater assessed through pyrolysis, kinetics and thermodynamics study to design algal biorefinery. *Bioresour Technol* 289:121701. <https://doi.org/10.1016/j.biortech.2019.121701>
- SNSA (2019) Brazilian secretary of environment sanitation. Brazilian sanitation information system: diagnosis of water and sewage services – 2017. <<http://www.snis.gov.br/diagnostico-agua-e-esgotos/diagnostico-ae-2017>> (accessed 01.08.19). 1–226
- Sawatdeenarunat C, Surendra KC, Takara D, Oechsner H, Khanal SK (2015) Anaerobic digestion of lignocellulosic biomass: challenges and opportunities. *Bioresour Technol* 178:178–186. <https://doi.org/10.1016/j.biortech.2014.09.103>
- Berni M, Dorileo I, Nathia G, Forster-Carneiro T, Lachos D, Santos BGM (2014) Anaerobic digestion and biogas production: combine effluent treatment with energy generation in UASB reactor as biorefinery annex. *Int J Chem Eng* 2014:1–8. <https://doi.org/10.1155/2014/543529>
- Barbosa RA, Sant'Anna GL (1989) Treatment of raw domestic sewage in an UASB reactor. *Water Res* 23:1483–1490. [https://doi.org/10.1016/0043-1354\(89\)90112-7](https://doi.org/10.1016/0043-1354(89)90112-7)
- Foresti E (2002) Anaerobic treatment of domestic sewage: established technologies and perspectives. *Water Sci Technol* 45:181–186. <https://doi.org/10.2166/wst.2002.0324>
- Vieira SMM, Carvalho JL, Barijan FPO, Rech CM (1994) Application of the UASB technology for sewage treatment in a small community at Sumare, Sao Paulo State. *Water Sci Technol* 30:203–210
- de Oliveira SJ, Filho GR, da Silva Meireles C et al (2012) Thermal analysis and FTIR studies of sewage sludge produced in treatment plants. The case of sludge in the city of Uberlândia-MG, Brazil. *Thermochim Acta* 528:72–75. <https://doi.org/10.1016/j.tca.2011.11.010>
- Samolada MC, Zabaniotou AA (2014) Comparative assessment of municipal sewage sludge incineration, gasification and pyrolysis for a sustainable sludge-to-energy management in Greece. *Waste Manag* 34:411–420. <https://doi.org/10.1016/j.wasman.2013.11.003>
- Syed-Hassan SSA, Wang Y, Hu S, Su S, Xiang J (2017) Thermochemical processing of sewage sludge to energy and fuel: fundamentals, challenges and considerations. *Renew Sust Eng Rev* 80:888–913. <https://doi.org/10.1016/j.rser.2017.05.262>
- Batistella L, Silva V, Suzin RC, Virmond E, Althoff CA, Moreira RFP, José HJ (2015) Gaseous emissions from sewage sludge combustion in a moving bed combustor. *Waste Manag* 46:430–439. <https://doi.org/10.1016/j.wasman.2015.08.039>
- Borges NB, Campos JR, Pablos JM (2015) Characterization of residual sand removed from the grit chambers of a wastewater treatment plant and its use as fine aggregate in the preparation of non-structural concrete. *Water Pract Technol* 10:164–171. <https://doi.org/10.2166/wpt.2015.018>
- Luque L, Westerhof R, Van Rossum G et al (2014) Pyrolysis based bio-refinery for the production of bioethanol from demineralized ligno-cellulosic biomass. *Bioresour Technol* 161:20–28. <https://doi.org/10.1016/j.biortech.2014.03.009>
- Mills N, Pearce P, Farrow J, Thorpe RB, Kirkby NF (2014) Environmental & economic life cycle assessment of current & future sewage sludge to energy technologies. *Waste Manag* 34:185–195. <https://doi.org/10.1016/j.wasman.2013.08.024>
- Alves JLF, Da Silva JCG, da Silva Filho VF et al (2019) Bioenergy potential of red macroalgae *Gelidium floridanum* by pyrolysis: evaluation of kinetic triplet and thermodynamics parameters. *Bioresour Technol* 291:121892. <https://doi.org/10.1016/j.biortech.2019.121892>
- Naqvi SR, Tariq R, Hameed Z, Ali I, Naqvi M, Chen WH, Ceylan S, Rashid H, Ahmad J, Taqvi SA, Shahbaz M (2019) Pyrolysis of high ash sewage sludge: kinetics and thermodynamic analysis using Coats-Redfern method. *Renew Energy* 131:854–860. <https://doi.org/10.1016/j.renene.2018.07.094>
- Vyazovkin S, Burnham AK, Criado JM, Pérez-Maqueda LA, Popescu C, Sbirrazzuoli N (2011) ICTAC kinetics committee recommendations for performing kinetic computations on thermal analysis data. *Thermochim Acta* 520:1–19. <https://doi.org/10.1016/j.tca.2011.03.034>
- da Silva Filho VF, Batistella L, Alves JLF, da Silva JCG, Althoff CA, Moreira RFP, José HJ (2019) Evaluation of gaseous emissions from thermal conversion of a mixture of solid municipal waste and wood chips in a pilot-scale heat generator. *Renew Energy* 141:402–410. <https://doi.org/10.1016/j.renene.2019.04.032>
- Mehmood MA, Ahmad MS, Liu Q, Liu CG, Tahir MH, Aloqbi AA, Tarbiah NI, Alsufiani HM, Gull M (2019) Helianthus tuberosus as a promising feedstock for bioenergy and chemicals appraised through pyrolysis, kinetics, and TG-FTIR-MS based study. *Energy Convers Manag* 194:37–45. <https://doi.org/10.1016/j.enconman.2019.04.076>
- Dhyani V, Kumar J, Bhaskar T (2017) Thermal decomposition kinetics of sorghum straw via thermogravimetric analysis. *Bioresour Technol* 245:1122–1129. <https://doi.org/10.1016/j.biortech.2017.08.189>
- Shahbeig H, Nosrati M (2020) Pyrolysis of municipal sewage sludge for bioenergy production: thermo-kinetic studies, evolved gas analysis, and techno-socio-economic assessment. *Renew Sust Eng Rev* 119:109567. <https://doi.org/10.1016/j.rser.2019.109567>
- Languer MP, Batistella L, Alves JLF, da Silva JCG, da Silva Filho VF, di Domenico M, Moreira RFP, José HJ (2020) Insights into pyrolysis characteristics of Brazilian high-ash sewage sludges using thermogravimetric analysis and bench-scale experiments with GC-MS to evaluate their bioenergy potential. *Biomass Bioenergy* 138:105614. <https://doi.org/10.1016/j.biombioe.2020.105614>
- Folgueras MB, Alonso M, Díaz RM (2013) Influence of sewage sludge treatment on pyrolysis and combustion of dry sludge. *Energy* 55:426–435. <https://doi.org/10.1016/j.energy.2013.03.063>
- Shao J, Yan R, Chen H, Wang B, Lee DH, Liang DT (2008) Pyrolysis characteristics and kinetics of sewage sludge by thermogravimetry Fourier transform infrared analysis. *Energy Fuel* 22:38–45. <https://doi.org/10.1021/ef700287p>
- Vyazovkin S, Burnham AK, Favregeon L, Koga N, Moukhina E, Pérez-Maqueda LA, Sbirrazzuoli N (2020) ICTAC Kinetics Committee recommendations for analysis of multi-step kinetics. *Thermochim Acta* 689:178597. <https://doi.org/10.1016/j.tca.2020.178597>
- Alves JLF, Da Silva JCG, da Silva Filho VF et al (2019) Determination of the bioenergy potential of Brazilian pine-fruit shell via pyrolysis kinetics, thermodynamic study, and evolved gas analysis. *Bioenergy Res* 12:168–183. <https://doi.org/10.1007/s12155-019-9964-1>
- Domenico MD, Amorim SM, Collazzo GC, José HJ, Moreira RFP (2019) Coal gasification in the presence of lithium orthosilicate. Part 1: reaction kinetics. *Chem Eng Res Des* 141:529–539. <https://doi.org/10.1016/j.cherd.2018.11.011>
- Uyar T, Suyadal Y (2019) Deactivation kinetics for lignite gasification in a fluidized bed reactor. *Fuel* 236:1050–1056. <https://doi.org/10.1016/j.fuel.2018.09.028>
- Thipkhanthod P, Meeyoo V, Rangsunvigit P, Kitiyanan B, Siemanond K, Rirksomboon T (2006) Pyrolytic characteristics of sewage sludge. *Chemosphere* 64:955–962. <https://doi.org/10.1016/j.chemosphere.2006.01.002>

30. Fonts I, Azuara M, Gea G, Murillo MB (2009) Study of the pyrolysis liquids obtained from different sewage sludge. *J Anal Appl Pyrolysis* 85:184–191. <https://doi.org/10.1016/j.jaap.2008.11.003>
31. García R, Pizarro C, Lavín AG, Bueno JL (2012) Characterization of Spanish biomass wastes for energy use. *Bioresour Technol* 103:249–258. <https://doi.org/10.1016/j.biortech.2011.10.004>
32. Ahmad MS, Mehmood MA, Luo H, Shen B, Latif M, Ghani WAWAK, Alkhatabi NA, Aloqbi AA, Jambi EJ, Gull M, Rashid U (2019) Pyrolysis and Thermogravimetric study to elucidate the bioenergy potential of novel feedstock produced on poor soils while keeping the environmental sustainability intact. *Sustainability* 11:3592. <https://doi.org/10.3390/su11133592>
33. Ahmad MS, Mehmood MA, Liu C-G, Tawab A, Bai FW, Sakdaronnarong C, Xu J, Rahimuddin SA, Gull M (2018) Bioenergy potential of *Wolffia arrhiza* appraised through pyrolysis, kinetics, thermodynamics parameters and TG-FTIR-MS study of the evolved gases. *Bioresour Technol* 253:297–303. <https://doi.org/10.1016/j.biortech.2018.01.033>
34. Yao Z, Yu S, Su W, Wu W, Tang J, Qi W (2020) Kinetic studies on the pyrolysis of plastic waste using a combination of model-fitting and model-free methods. *Waste Manag Res* 38:77–85. <https://doi.org/10.1177/0734242X19897814>
35. Yao Z, Yu S, Su W, Wu W, Tang J, Qi W (2020) Comparative study on the pyrolysis kinetics of polyurethane foam from waste refrigerators. *Waste Manag Res* 38:271–278. <https://doi.org/10.1177/0734242X19877682>
36. Konwar K, Nath HP, Bhuyan N, Saikia BK, Borah RC, Kalita AC, Saikia N (2019) Effect of biomass addition on the devolatilization kinetics, mechanisms and thermodynamics of a northeast Indian low rank sub-bituminous coal. *Fuel* 256:115926. <https://doi.org/10.1016/j.fuel.2019.115926>
37. Tahir MH, Çakman G, Goldfarb JL, Topcu Y, Naqvi SR, Ceylan S (2019) Demonstrating the suitability of canola residue biomass to biofuel conversion via pyrolysis through reaction kinetics, thermodynamics and evolved gas analyses. *Bioresour Technol* 279:67–73. <https://doi.org/10.1016/j.biortech.2019.01.106>
38. Hu M, Chen Z, Wang S, Guo D, Ma C, Zhou Y, Chen J, Laghari M, Fazal S, Xiao B, Zhang B, Ma S (2016) Thermogravimetric kinetics of lignocellulosic biomass slow pyrolysis using distributed activation energy model, Fraser–Suzuki deconvolution, and iso-conversional method. *Energy Convers Manag* 118:1–11. <https://doi.org/10.1016/j.enconman.2016.03.058>
39. Alves JLF, Da Silva JCG, Costa RL et al (2019) Investigation of the bioenergy potential of microalgae *Scenedesmus acuminatus* by physicochemical characterization and kinetic analysis of pyrolysis. *J Therm Anal Calorim* 135:3269–3280. <https://doi.org/10.1007/s10973-018-7506-2>
40. Alves JLF, da Silva JCG, da Silva Filho VF, Alves RF, de Araujo Galdino WV, de Sena RF (2019) Kinetics and thermodynamics parameters evaluation of pyrolysis of invasive aquatic macrophytes to determine their bioenergy potentials. *Biomass Bioenergy* 121:28–40. <https://doi.org/10.1016/j.biombioe.2018.12.015>
41. Monlau F, Sambusiti C, Antoniou N, Barakat A, Zabaniotou A (2015) A new concept for enhancing energy recovery from agricultural residues by coupling anaerobic digestion and pyrolysis process. *Appl Energy* 148:32–38. <https://doi.org/10.1016/j.apenergy.2015.03.024>

**Publisher's Note** Springer Nature remains neutral with regard to jurisdictional claims in published maps and institutional affiliations.